EXPERIMENTAL PROCEDURE FOR IDENTIFYING YIELD CRITERIA FOR POWDER MATERIALS AND ITS IMPLEMENTATION

Sergei Alexandrov[1,2], Yeong-Maw Hwang[3*], Elena Lyamina[1], and Jun-Ru Chen[3]

[1] *Ishlinsky Institute for Problems in Mechanics RAS, 101-1 Prospect Vernadskogo, Moscow 119526, Russia*
[2] *RUDN University, 6 Miklukho-Maklaya St., Moscow 117198, Russia*
[3] *Department of Mechanical and Electro-Mechanical Engineering, National Sun Yat-sen University, Lien-Hai Rd., Kaohsiung 804, Taiwan*
[*] *Corresponding author. E-mail: ymhwang@mail.nsysu.edu.tw*

Received: Nov. 28, 2023; Accepted: Jul. 25, 2024

This paper is devoted to developing an experimental/theoretical procedure for identifying yield criteria for powder materials. The experimental part includes several compression tests. The variation of the loading paths in these tests is achieved by deforming a plastically incompressible ring and powder material together. The description of the ring's material behavior is not required to interpret experimental results, which is an advantage of the proposed method. The theoretical description of the test is provided using an analytical solution, which is also an advantage of the proposed method. The method is adopted for identifying Green's yield criterion for aluminum powder. Comparison with other predictions of the yield criterion for this material is made.

Keywords: powder materials; yield criterion; compression tests; plasticity theory.

http://dx.doi.org/10.6180/jase.202507_28(7).0004

1. Introduction

The phenomenological theory of plasticity is an efficient tool for modeling the deformation processes, including the deformation of powder and porous materials. A full account of this theory for the latter materials has been provided in [1]. Several non-standard issues of the theory have been considered in [2]. In most cases, neglecting the elastic component of the strain is a reasonable assumption. The yield criterion fully determines the material behavior if the associated flow rule is accepted. Therefore, the yield criterion's accuracy controls theoretical solutions' accuracy.

Several yield criteria for powder and porous materials are available in the literature. Reviews of such yield criteria can be found in [1, 3, 4]. The most widely used criteria have been proposed in [5, 6]. Like any other yield criteria for powder and porous materials, these yield criteria depend on porosity or relative density. It is a challenging task to identify this dependence. One method for this is purely theoretical. This method considers a representative volume element that consists of a pore (or pores) in a plastically incompressible material. The element is subjected to various loading paths, which allows a yield criterion to be calculated using analytical or numerical solutions [5–12]. The effect of non-uniform pore distribution of the yield criterion has been investigated in [13]. Paper [14] has shown that the Tsai-Hill failure criterion for transversely isotropic materials under plane stress conditions can be used as a yield criterion. The plastically incompressible matrix's material behavior is assumed and is supposed to be determined from independent experiments. However, it has been pointed out in [15] that the mechanical properties of powder materials are usually different from those of the corresponding wrought material, which requires different testing procedures. The other method is purely experimental. This method assumes a yield criterion involving

arbitrary functions of the relative density and determines these functions through a series of tests. Paper [16] has utilized the purely experimental method in conjunction with the yield criterion proposed in [5].

The present paper is partly based on the approach developed in [16]. However, there are essential differences. In particular, the test procedure in [16] has been applied to sintered porous materials and included tension tests. Therefore, it is not feasible for powder materials. The procedure proposed in the present paper consists of several compression tests that generate different loading paths in the powder material tested. The geometry of the tests is very simple, which permits its analytical description. The variation of the loading paths is achieved by deforming together a plastically incompressible ring and the powder material. The description of the ring's material behavior is not required to interpret experimental results, which is an advantage of the proposed method.

2. Design of experiment

A schematic diagram of the proposed axisymmetric upsetting test is shown in Fig. 1. For the description of this test, it is convenient to use a cylindrical coordinate system (r, θ, z) whose z -axis coincides with the axis of process symmetry and the plane $z = 0$ with the bottom of the die. The test setup consists of a closed die, a punch, a ring made of plastically incompressible material, and powder whose yield criterion is under investigation. It is assumed that friction is negligible. The ring's outer radius and the die's radius are R_0, and the initial inner radius of the ring is r_0. The initial height of the ring is H_0. The powder occupies the domain $0 \le r \le r_0$ and $0 \le z \le H_0$. The punch compresses both the ring and powder material. As the deformation proceeds, the ring's inner radius decreases. This deformation of the ring imposes additional loading on the powder material. Therefore, choosing different values of r_0 can create different stress fields in the powder material, allowing for a portion of the yield surface to be determined. It will be shown below that plastic incompressibility is the only property of the ring's material required for interpreting experimental results.

The current inner radius of the ring is denoted as r_c, and its current height is H (Fig. 1(b)). Since the ring is plastically incompressible,

$$H_0\left(R_0^2 - r_0^2\right) = H\left(R_0^2 - r_c^2\right). \tag{1}$$

In what follows, it is convenient to use the following dimensionless quantities:

$$h = \frac{H}{H_0}, \quad h_0 = \frac{H_0}{R_0}, \quad \zeta = \frac{z}{H_0}, \quad \rho = \frac{r}{R_0}, \quad s = \frac{r_c}{R_0}, \quad \text{and} \quad s_0 = \frac{r_0}{R_0}. \tag{2}$$

Then, Eq. (1) becomes

$$h\left(1 - s^2\right) = 1 - s_0^2. \tag{3}$$

Let σ_r, σ_θ, and σ_z be the normal stresses in the cylindrical coordinate system. Since friction is neglected, these stresses are the principal stresses. The experimental procedure consists of two steps for each value of s_0. The first step is to compress the ring with no powder, and the second is to compress the ring with its hole filled with the powder. Let $F_R(h)$ be the dependence of the compression force on h determined during the first step. The radial and axial stresses of the stress field that produces this force are denoted as $\sigma_r^{(0)}$ and $\sigma_z^{(0)}$, respectively. The superscript ' 0 ' emphasizes that this stress field appears in the ring compressed with no powder. This stress field must satisfy the following condition:

$$\sigma_r^{(0)} = 0 \tag{4}$$

for $\rho = s$. The force $F_R(h)$ can be represented as

$$F_R(h) = 2\pi \int_{r_c}^{R_0} \left|\sigma_z^{(0)}\right| r dr \tag{5}$$

It is understood here that the stress $\sigma_z^{(0)}$ is calculated at $z = H$. Using Eq. (2), one can rewrite Eq. (5) in the form

$$F_R(h) = 2\pi R_0^2 \int_s^1 \left|\sigma_z^{(0)}\right| \rho d\rho. \tag{6}$$

One may superimpose uniform hydrostatic pressure on the stress field in the ring without violating the equilibrium and constitutive equations if the ring's material obeys a model of pressure-independent plasticity. The radial and axial stresses become $\sigma_r = \sigma_r^{(0)} - q_0$ and $\sigma_z = \sigma_z^{(0)} - q_0$, where q_0 is independent of space coordinates but depends on h . The condition Eq. (4) is replaced with

$$\sigma_r = -q_0 \tag{7}$$

for $\rho = s$. The force produced by the auxiliary stress field over the plane $z = H$ is

$$F_A(h) = 2\pi \int_{r_c}^{R_0} \left(\left|\sigma_z^{(0)}\right| + q_0\right) r dr. \tag{8}$$

Using Eqs. (2) and (6), one transforms this equation to

$$F_A(h) = F_R(h) + \pi R_0^2 q_0 \left(1 - s^2\right). \tag{9}$$

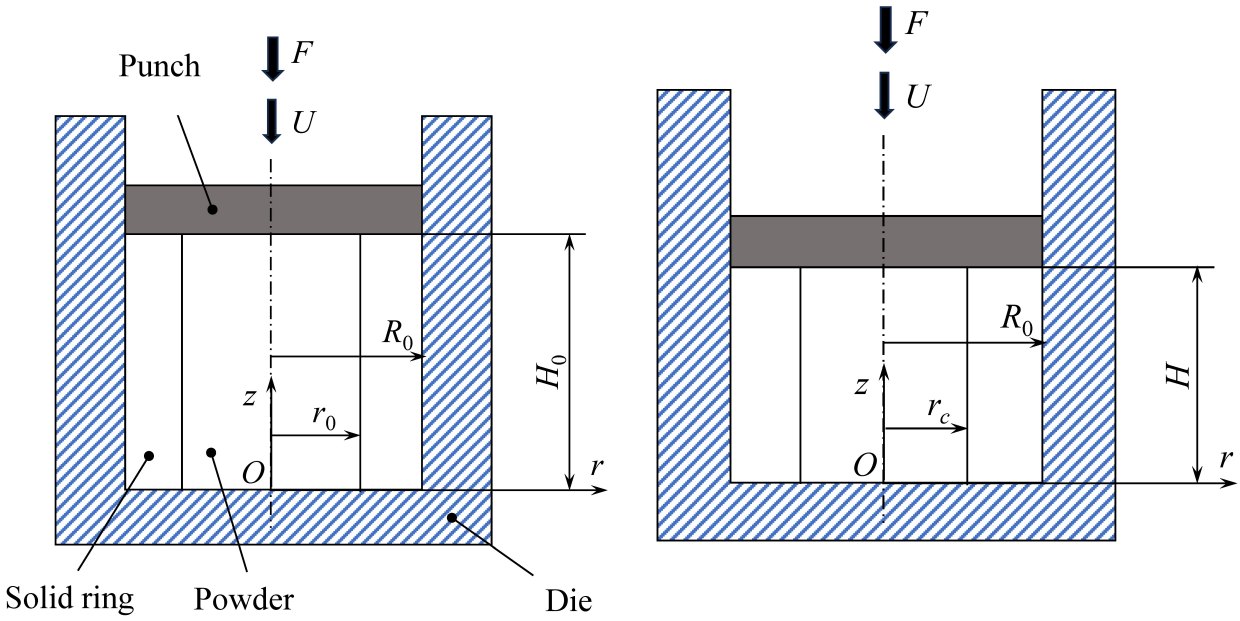

Fig. 1. Schematic diagram of the process: (a) initial instant, (b) after any amount of deformation.

Eliminating s in this equation employing Eq. (3), one gets

$$F_A(h) = F_R(h) + \frac{\pi R_0^2 q_0 \left(1 - s_0^2\right)}{h}. \tag{10}$$

If one can connect q_0 to the yield criterion for the powder material, equation Eq. (10) provides the basis for identifying this criterion. It requires a solution in the domain occupied by the powder material.

3. Solution for the powder material

3.1. Material model

The elastic component of the strain is neglected. The yield criterion is assumed to be

$$\Phi\left(I_1, I_2, \vartheta\right) = \sigma_0^2. \tag{11}$$

Here I_1 is the linear invariant of the stress tensor, I_2 is the quadratic invariant of the stress tensor, ϑ is the relative density, and σ_0 is a reference stress. Also, $\Phi\left(I_1, I_2, \vartheta\right)$ is an arbitrary function of its arguments satisfying the standard requirements imposed on the yield criteria. The stress invariants are defined as

$$\begin{aligned} &I_1 = \sigma_1 + \sigma_2 + \sigma_3 \quad \text{and} \\ &I_2 = \sqrt{(\sigma_1 - \sigma_2)^2 + (\sigma_2 - \sigma_3)^2 + (\sigma_3 - \sigma_1)^2}, \end{aligned} \tag{12}$$

where σ_1, σ_2, and σ_3 are the principal stresses. Let ξ_1, ξ_2, and ξ_3 be the principal strain rates. The plastic flow rule associated with the yield criterion Eq. (11) is

$$\begin{aligned} \xi_1 &= \lambda \left[\frac{\partial \Phi}{\partial I_1} + \frac{(2\sigma_1 - \sigma_2 - \sigma_3)}{I_2} \frac{\partial \Phi}{\partial I_2}\right], \\ \xi_2 &= \lambda \left[\frac{\partial \Phi}{\partial I_1} + \frac{(2\sigma_2 - \sigma_3 - \sigma_1)}{I_2} \frac{\partial \Phi}{\partial I_2}\right], \\ \xi_3 &= \lambda \left[\frac{\partial \Phi}{\partial I_1} + \frac{(2\sigma_3 - \sigma_1 - \sigma_2)}{I_2} \frac{\partial \Phi}{\partial I_2}\right], \end{aligned} \tag{13}$$

where $\lambda \geq 0$.

The constitutive equations above must be supplemented by the stress equilibrium equations and the continuity equation. The latter can be represented in the form

$$\frac{d\vartheta}{dt} + \vartheta\left(\xi_1 + \xi_2 + \xi_3\right) = 0, \tag{14}$$

where d/dt denotes the material derivative.

3.2. Initial and boundary conditions

A cylinder of powder material is compressed in the axial direction. The initial relative density is ϑ_0. The boundary condition in Eq. (7) is valid. The speed of the punch is U. Therefore, $dH/dt = -U$. Using Eq. (2), one transforms this equation to

$$\frac{dh}{dt} = -\frac{U}{H_0}. \tag{15}$$

Let u_r and u_z be the radial and axial velocities. By definition, $u_r = dr_c/dt$ at $r = r_c$. Using Eqs. (2) and (15), one

transforms this equation to

$$u_r = -\frac{U}{h_0}\frac{ds}{dh} \tag{16}$$

for $\rho = s$. Differentiating Eq. (3) with respect to h yields

$$\frac{ds}{dh} = \frac{1-s^2}{2hs}. \tag{17}$$

Substituting Eq. (17) into Eq. (16) gives

$$u_r = -\frac{U\left(1-s^2\right)}{2h_0 hs} \tag{18}$$

for $\rho = s$. The other velocity boundary conditions are

$$u_r = 0 \tag{19}$$

for $\rho = 0$,

$$u_z = 0 \tag{20}$$

for $\zeta = 0$, and

$$u_z = -U \tag{21}$$

for $\zeta = h$.

3.3. Solution

An inverse method widely used in plasticity is employed for finding the solution in the domain occupied by the powder material. Neglecting friction suggests uniform distributions of the stress and strain rate components. A suitable velocity field satisfying the boundary conditions Eq. (18) to Eq. (21) is

$$u_z = -\frac{U\zeta}{h} \quad \text{and} \quad u_r = -\frac{U\left(1-s^2\right)}{2h_0 hs^2}\rho. \tag{22}$$

Then, the normal strain rates in the cylindrical coordinate system are

$$\begin{aligned} &\xi_r = -\frac{U}{2H_0}\frac{\left(1-s^2\right)}{hs^2}, \quad \xi_\theta = -\frac{U}{2H_0}\frac{\left(1-s^2\right)}{hs^2}, \\ &\text{and} \quad \xi_z = -\frac{U}{H_0 h}. \end{aligned} \tag{23}$$

One can put without loss of generality that $\xi_r \equiv \xi_1, \xi_\theta \equiv \xi_2$, and $\xi_z \equiv \xi_3$. Then, $\sigma_r \equiv \sigma_1$, $\sigma_\theta \equiv \sigma_2$, and $\sigma_z \equiv \sigma_3$. Substituting Eq. (23) into Eq. (13) yields

$$\begin{aligned} -\frac{U}{2H_0}\frac{\left(1-s^2\right)}{hs^2} &= \lambda\left[\frac{\partial\Phi}{\partial I_1} + \frac{(2\sigma_r-\sigma_\theta-\sigma_z)}{I_2}\frac{\partial\Phi}{\partial I_2}\right] \\ -\frac{U}{2H_0}\frac{\left(1-s^2\right)}{hs^2} &= \lambda\left[\frac{\partial\Phi}{\partial I_1} + \frac{(2\sigma_\theta-\sigma_z-\sigma_r)}{I_2}\frac{\partial\Phi}{\partial I_2}\right], \\ -\frac{U}{H_0 h} &= \lambda\left[\frac{\partial\Phi}{\partial I_1} + \frac{(2\sigma_z-\sigma_r-\sigma_\theta)}{I_2}\frac{\partial\Phi}{\partial I_2}\right]. \end{aligned} \tag{24}$$

The first two equations show that

$$\sigma_r = \sigma_\theta. \tag{25}$$

Using this equation and eliminating λ between the second and third equations in Eq. (24) results in

$$\frac{\left(1-s^2\right)}{2s^2} = \left[\frac{\partial\Phi}{\partial I_1} + \frac{(\sigma_r-\sigma_z)}{I_2}\frac{\partial\Phi}{\partial I_2}\right]\left[\frac{\partial\Phi}{\partial I_1} + \frac{2\,(\sigma_z-\sigma_r)}{I_2}\frac{\partial\Phi}{\partial I_2}\right]^{-1}. \tag{26}$$

The boundary condition Eq. (7) is satisfied by putting

$$\sigma_r = -q_0 = -q\sigma_0 \tag{27}$$

everywhere in the powder material. The corresponding value of σ_z is denoted as $-p\sigma_0$.

Then, equations Eqs. (11), (12) and (26) become

$$I_1 = -(2q+p)\sigma_0, \quad I_2 = \sqrt{2}(p-q)\sigma_0, \tag{28}$$

$$\Phi\left[-(2q+p)\sigma_0, \sqrt{2}(p-q)\sigma_0, \vartheta\right] = \sigma_0^2 \tag{29}$$

and

$$\frac{\left(1-s^2\right)}{2s^2} = \left[\frac{\partial\Phi}{\partial I_1} + \frac{1}{\sqrt{2}}\frac{\partial\Phi}{\partial I_2}\right]\left[\frac{\partial\Phi}{\partial I_1} - \sqrt{2}\frac{\partial\Phi}{\partial I_2}\right]^{-1}. \tag{30}$$

The second equation in Eq. (28) is valid if

$$p > q. \tag{31}$$

This inequality should be verified a posteriori. Using Eq. (3), one can transform Eq. (30) to

$$\frac{\left(1-s_0^2\right)}{2\left(h-1+s_0^2\right)} = \left[\frac{\partial\Phi}{\partial I_1} + \frac{1}{\sqrt{2}}\frac{\partial\Phi}{\partial I_2}\right]\left[\frac{\partial\Phi}{\partial I_1} - \sqrt{2}\frac{\partial\Phi}{\partial I_2}\right]^{-1}. \tag{32}$$

Eqs. (29) and (32) compose the system for determining p and q if ϑ is known. This system is compatible if the distribution of ϑ is uniform.

Assuming that the distribution of ϑ is uniform, Eq. (14) becomes $\vartheta_0 H_0 r_0^2 = \vartheta H r_c^2$. Using Eqs. (2) and (3), one can rewrite this equation as

$$\vartheta = \frac{\vartheta_0 s_0^2}{h-1+s_0^2}. \tag{33}$$

The total compression force is

$$F(h) = F_A(h) + \frac{\pi R_0^2 \sigma_0 p\left(h-1+s_0^2\right)}{h}. \tag{34}$$

Here Eqs. (2) and (3) have been used. Eliminating $F_A(h)$ employing Eq. (10), one gets

$$F(h) = F_R(h) + \frac{\pi R_0^2 \sigma_0 \left[p\left(h - 1 + s_0^2\right) + q\left(1 - s_0^2\right)\right]}{h}. \quad (35)$$

In this equation, $F_A(h)$ and $F(h)$ are known from the experiment. Equation Eq. (29) allows q (or p) to be eliminated in Eq. (35). The resulting equation determines p (or q) as a function of h.

Using Eq. (33), one can transform this function into a function of ϑ. It is convenient to rewrite Eq. (35) in the following dimensionless form:

$$f(h) = f_R(h) + \frac{p\left(h - 1 + s_0^2\right) + q\left(1 - s_0^2\right)}{h}, \quad (36)$$

where

$$f(h) = \frac{F(h)}{\pi R_0^2 \sigma_0} \quad \text{and} \quad f_R(h) = \frac{F_R(h)}{\pi R_0^2 \sigma_0}. \quad (37)$$

4. Green's yield criterion

The yield criterion proposed in [5] is obtained from Eq. (11) if

$$\Phi\left(I_1, I_2, \vartheta\right) = g_1(\vartheta) I_1^2 + g_2(\vartheta) I_2^2, \quad (38)$$

where $g_1(\vartheta)$ and $g_2(\vartheta)$ are the functions of the relative density. These functions must satisfy the following conditions:

$$g_1(\vartheta) = 0 \quad \text{and} \quad g_2(\vartheta) = \frac{1}{2} \quad (39)$$

at $\vartheta = 1$. The second condition is valid if the pore-free material obeys the von Mises yield criterion and σ_0 is the tensile yield stress of this material.

The derivatives $\partial\Phi/\partial I_1$ and $\partial\Phi/\partial I_2$ involved in Eq. (32) are determined from Eq. (38) as

$$\frac{\partial \Phi}{\partial I_1} = 2 g_1(\vartheta) I_1 \quad \text{and} \quad \frac{\partial \Phi}{\partial I_2} = 2 g_2(\vartheta) I_2. \quad (40)$$

Using Eq. (28), one can transform these equations to

$$\frac{\partial \Phi}{\partial I_1} = -2 g_1(\vartheta)(2q + p)\sigma_0 \quad \text{and} \quad \frac{\partial \Phi}{\partial I_2} = 2\sqrt{2} g_2(\vartheta)(p - q)\sigma_0. \quad (41)$$

In the case of the yield criterion Eq. (38), Eq. (29) becomes

$$g_1(\vartheta)(2q + p)^2 + 2 g_2(\vartheta)(p - q)^2 = 1. \quad (42)$$

Substituting Eq. (41) into Eq. (32) gives

$$\frac{\left(1 - s_0^2\right)}{2\left(h - 1 + s_0^2\right)} = \frac{(2q + p) g_1(\vartheta) - (p - q) g_2(\vartheta)}{(2q + p) g_1(\vartheta) + 2(p - q) g_2(\vartheta)} \quad (43)$$

The left-hand side of this equation can be transformed into a function of the relative density using Eq. (33). As a result,

$$\frac{\left(1 - s_0^2\right)\vartheta}{2\vartheta_0 s_0^2} = \frac{(2q + p) g_1(\vartheta) - (p - q) g_2(\vartheta)}{(2q + p) g_1(\vartheta) + 2(p - q) g_2(\vartheta)}. \quad (44)$$

One can solve Eqs. (42) and (44) for p and q to get

$$p = \frac{1}{3\sqrt{g_2}}\left(\frac{\cos\gamma}{k} + \sqrt{2}\sin\gamma\right) \quad \text{and} \quad q = \frac{1}{3\sqrt{g_2}}\left(\frac{\cos\gamma}{k} - \frac{\sin\gamma}{\sqrt{2}}\right), \quad (45)$$

where

$$k = \sqrt{\frac{g_1}{g_2}}, \quad \gamma = \arctan\left[\frac{\sqrt{2}k(1 - \Lambda)}{1 + 2\Lambda}\right], \quad \text{and} \quad \Lambda(\vartheta) = \frac{\left(1 - s_0^2\right)\vartheta}{2\vartheta_0 s_0^2}. \quad (46)$$

It follows from Eq. (39) that

$$k = 0 \quad (47)$$

at $\vartheta = 1$. Using Eq. (33), one can rewrite equation Eq. (36) as

$$t(\vartheta) - t_R(\vartheta) = \left[\frac{p\vartheta_0 s_0^2}{\vartheta} - q\left(1 - s_0^2\right)\right]\left(\frac{\vartheta_0 s_0^2}{\vartheta} + 1 - s_0^2\right)^{-1}, \quad (48)$$

where

$$t(\vartheta) = f\left(\frac{\vartheta_0 s_0^2}{\vartheta} + 1 - s_0^2\right) \quad \text{and} \quad t_R(\vartheta) = f_R\left(\frac{\vartheta_0 s_0^2}{\vartheta} + 1 - s_0^2\right). \quad (49)$$

The functions $t(\vartheta), t_R(\vartheta), p(\vartheta)$, and $q(\vartheta)$ depend on the process (i.e., they involve s_0), whereas the functions $g_1(\vartheta)$ and $g_2(\vartheta)$ do not. To emphasize the process-dependence of the former group of functions, the new notation for these functions is $t^{(i)}(\vartheta), t_R^{(i)}(\vartheta), p^{(i)}(\vartheta)$, and $q^{(i)}(\vartheta)$. Here different numbers i correspond to different processes.

In the special case of the upsetting without the ring, $s = s_0 = 1$, and $f_R(h)$ vanishes. The superscript (0) will be used for this special case. Eq. (48) supplies

$$t^{(0)} = p^{(0)}. \quad (50)$$

Eq. (46) shows that $\Lambda = 0$. Therefore, Eq. (45) and Eq. (50) combine to give

$$t^{(0)} = \frac{1}{3\sqrt{g_2}}\left(\frac{\cos\gamma_0}{k} + \sqrt{2}\sin\gamma_0\right), \quad (51)$$

where $\gamma_0 = \arctan(\sqrt{2}k)$.

In a generic, non-special case, Eqs. (45) and (49) supply

$$\left[t^{(i)}(\vartheta) - t_R^{(i)}(\vartheta)\right] = \frac{1}{3\sqrt{g_1}}\left[\frac{\vartheta_0 s_0^2}{\vartheta}(\cos\gamma + \sqrt{2}k\sin\gamma) - \left(1 - s_0^2\right)\left(\cos\gamma - \frac{k}{\sqrt{2}}\sin\gamma\right)\right]\left(\frac{\vartheta_0 s_0^2}{\vartheta} + 1 - s_0^2\right)^{-1}. \tag{52}$$

Eqs. (50) and (52) combine to yield

$$w(\vartheta) = \frac{\left[\frac{\vartheta_0 s_0^2}{\vartheta}(\cos\gamma + \sqrt{2}k\sin\gamma) - \left(1 - s_0^2\right)\left(\cos\gamma - \frac{k}{\sqrt{2}}\sin\gamma\right)\right]}{\left(\frac{\vartheta_0 s_0^2}{\vartheta} + 1 - s_0^2\right)\left(\cos\gamma_0 + \sqrt{2}k\sin\gamma_0\right)} \tag{53}$$

where

$$w(\vartheta) = \frac{t^{(i)}(\vartheta) - t_R^{(i)}(\vartheta)}{t^{(0)}(\vartheta)} \tag{54}$$

Eq. (53) provides the relationship between k and the experimental data on its left-hand side. Once the dependence of k on the relative density has been found, Eq. (51) provides g_2 as

$$g_2(\vartheta) = \frac{1}{9\left[t^{(0)}\right]^2}\left(\frac{\cos\gamma_0}{k} + \sqrt{2}\sin\gamma_0\right)^2. \tag{55}$$

Note that the definition of $t^{(0)}$ involves σ_0, which is still undetermined. The second equation in Eq. (39) supplies the condition for determining this quantity.

It follows from Eq. (45) that the inequality in Eq. (31) is equivalent to

$$\sin\gamma > 0. \tag{56}$$

5. Experimental

The powder material tested was aluminum alloy AL-6061-T6. Teflon sheets were used to minimize friction on contact surfaces (Fig. 1). The die's radius was 15 mm . Two series of tests were carried out. One series tested the powder material without using the ring. The ring of inner radius 12 mm was used in the other series. The initial height of the powder cylinder was 40 mm in both series. Therefore, as follows from Eq. (2), the first series was classified by the following dimensionless parameters: $s_0 = 1$ and $h_0 = 8/3$, and the second series by $s_0 = 4/5$ and $h_0 = 8/3$. The initial relative density was $\vartheta_0 = 0.55$. The experiment was conducted according to the procedure described in Section 2.

Fig. 2 depicts the experimental dependencies of the compression force on the stroke. These experimental data were approximated by employing first-order polynomials to calculate $t(\vartheta)$ and $t_R(\vartheta)$ using (49). These dependencies are illustrated in Figure 3. They allow the right-hand side of (54) to be calculated, assuming that $t^{(i)}(\vartheta) = t^{(1)}(\vartheta)$ and $t_R^{(i)}(\vartheta) = t_R^{(1)}(\vartheta)$ correspond to $s_0 = 4/5$. Note that the value of σ_0 involved in the definition of $t^{(0)}(\vartheta)$, $t^{(1)}(\vartheta)$, and $t_R^{(1)}(\vartheta)$ is immaterial in this case because the ratio of the dimensionless forces is required in this calculation.

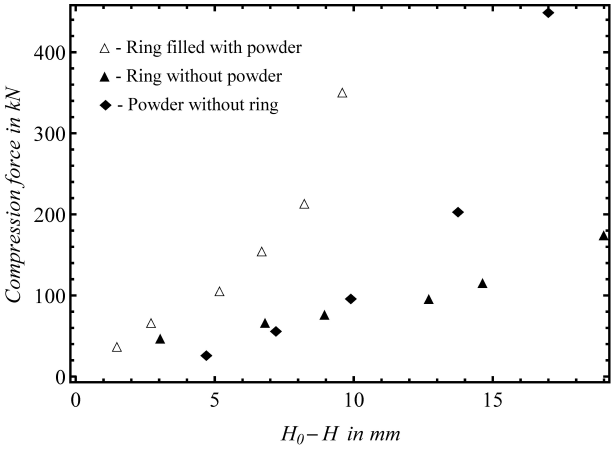

Fig. 2. Dependence of the experimental compression force on the stroke.

Eq. (53) can now be employed for determining k. This function was determined in [16] for sintered copper using another experimental procedure. The final result can be represented as

$$k = k^{(S)}(\vartheta) = 1.17(1 - \vartheta)^{0.514}. \tag{57}$$

It was hypothesized in [16] that Eq. (57) would be valid for sintered aluminum. Therefore, the present paper assumes that

$$k = k^{(S)}(\vartheta) + A(1 - \vartheta). \tag{58}$$

This function satisfies Eq. (47) at any value of A. The latter was found using the experimental data above and the least squares method. As a result, $A = 0.188$, and Eqs. (57) and (58) combine to give

$$k = 1.17(1 - \vartheta)^{0.514} + 0.188(1 - \vartheta). \tag{59}$$

Another equation for k can be derived by employing the theoretical solution provided in [4]. It is

$$k = k^{(G)}(\vartheta) = -\frac{3(1 - \sqrt[3]{1 - \vartheta})}{\sqrt{2}(3 - 2\sqrt[4]{1 - \vartheta})\ln(1 - \vartheta)}. \tag{60}$$

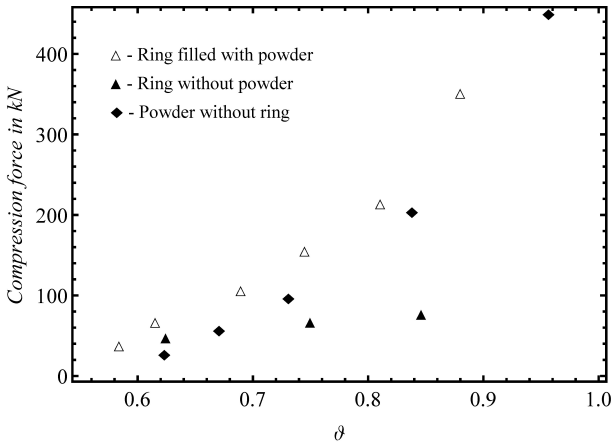

Fig. 3. Dependence of the experimental compression force on the average relative density.

It can be verified that $\lim_{\vartheta\to 1} k^{(G)}(\vartheta) = 0$. This theoretical solution can be modified to account for the experimental data as

$$k = k^{(G)}(\vartheta) + B(1-\vartheta). \tag{61}$$

This function satisfies Eq. (47) at any value of B. The latter was found using the experimental data above and the least squares method. As a result, $B = 1.03$, and Eqs. (60) and (61) combine to give

$$k = -\frac{3(1-\sqrt[3]{1-\vartheta})}{\sqrt{2}(3-2\sqrt[4]{1-\vartheta})\ln(1-\vartheta)} + 1.03(1-\vartheta). \tag{62}$$

Fig. 4 illustrates the above variations of k with the relative density (Curve 1 corresponds to $k^{(S)}(\vartheta)$, curve 2 to Eq. (59), curve 3 to $k^{(G)}(\vartheta)$, and curve 4 to Eq. (62)). It is seen that the scatter is rather large. Fig. 5 shows the left-hand side of Eq. (53) found using the experimental data (the discrete line) and its right-hand side calculated using the above dependencies of k on the relative density (Curve 1 corresponds to $k^{(S)}(\vartheta)$, curve 2 to Eq. (59), curve 3 to $k^{(G)}(\vartheta)$, and curve 4 to Eq. (62)). It is seen that the predictive capacity of the k-functions is reasonable except for $k^{(S)}(\vartheta)$.

Substituting k from Eq. (59) or Eq. (62) into Eq. (46), one can show numerically that the inequality in Eq. (56) is satisfied.

It is now necessary to determine the function $g_2(\vartheta)$. The difficulty here is that no experimental data can be used to directly satisfy the requirement formulated in the second equation in Eq. (39). It is, therefore, reasonable to approximate the experimental compression force $f(\vartheta) = t^{(0)}(\vartheta)$ first. In particular, Eq. (51) shows that $O\left[t^{(0)}(\vartheta)\right] = O\left(p^{(0)}\right)$ as $\vartheta \to 1$. Fig. 6 shows the experimental values of the compression force and its approximations based on Eqs. (59) and (62). All three curves practically coincide. In the course of this calculation, the value of σ_0 was also found. In particular, $\sigma_0 = 210$MPa. The function $g_2(\vartheta)$ is determined from Eq. (51). It can be accurately approximated as

$$g_2(\vartheta) = \frac{1}{2} + 0.48\tan^{2.5}\left[\frac{(1-\vartheta)}{0.28}\right]. \tag{63}$$

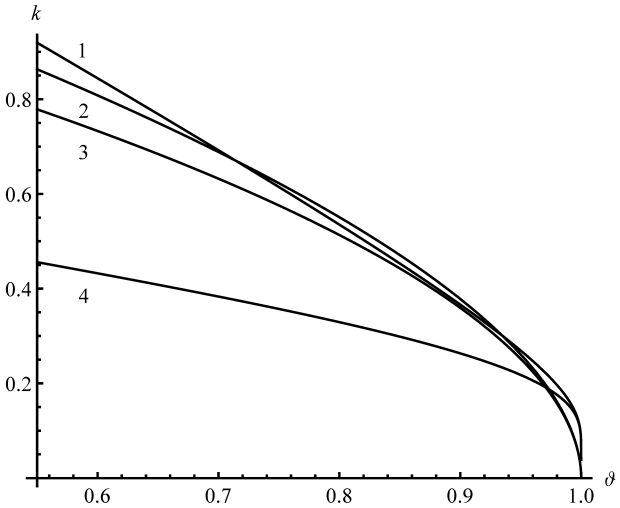

Fig. 4. Empirical dependencies of k on the relative density.

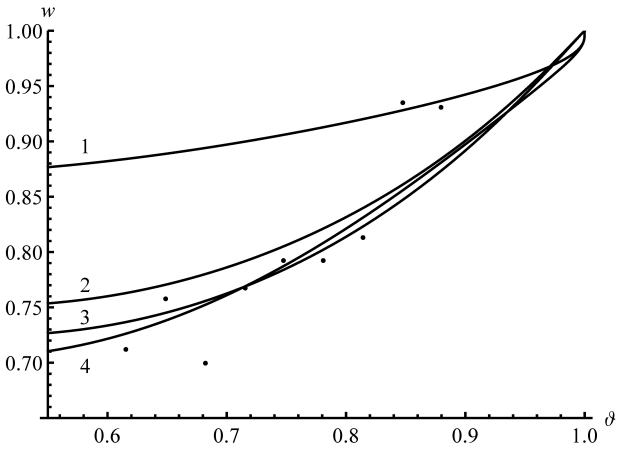

Fig. 5. Experimental dependence of w on the relative density and its empirical representations.

Two curves in Fig. 7 correspond to the function $g_2(\vartheta)$ calculated using the approximating functions for k and $t^{(0)}(\vartheta)$, and one corresponds to Eq. (63). All three curves practically coincide.

Using Eqs. (59), (62) and (63), one can rewrite Eq. (38) as

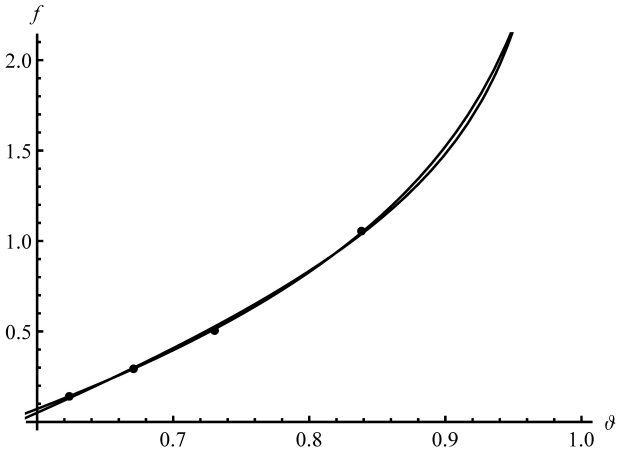

Fig. 6. Experimental dependence of the dimensionless compression force and its theoretical approximations for the compression of the powder material without the ring.

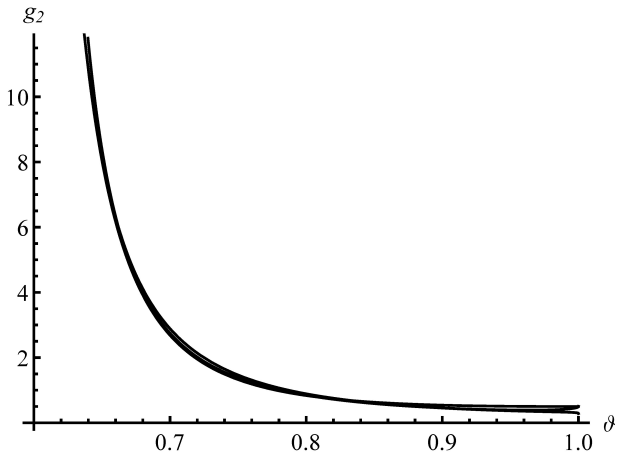

Fig. 7. Illustration of the behavior of the function $g_2(\vartheta)$.

$$\Phi\left(I_1, I_2, \vartheta\right) = \left\{\frac{1}{2} + 0.48\tan^{2.5}\left[\frac{(1-\vartheta)}{0.28}\right]\right\}\left\{I_2^2 + \left[1.17(1-\vartheta)^{0.514} + 0.188(1-\vartheta)\right]^2 I_1^2\right\} \tag{64}$$

or

$$\Phi\left(I_1, I_2, \vartheta\right) = \left\{\frac{1}{2} + 0.48\tan^{2.5}\left[\frac{(1-\vartheta)}{0.28}\right]\right\}\left\{I_2^2 + \left[-\frac{3(1-\sqrt[3]{1-\vartheta})}{\sqrt{2}(3-2\sqrt[4]{1-\vartheta})\ln(1-\vartheta)} + 1.03(1-\vartheta)\right]^2 I_1^2\right\}. \tag{65}$$

The yield criterion (11) can now be derived using the abovementioned σ_0- values. The range of the used experimental data suggests that Eqs. (64) and (65) are reliable for $\vartheta > 0.6$

6. Conclusions

This paper has proposed an experimental/theoretical procedure for identifying yield criteria that depend on the relative density and the linear and quadratic stress invariants. The experimental part requires the compression of a ring whose hole is filled in with the powder material tested. This part also includes the compression of the same ring without the powder material and the compression of the powder material without the ring. The advantages of the procedure are a simple theoretical description and the independence of the final result on the properties of the ring. The quality of the experimental data can be increased using rings with different initial inner radii. It is also possible to compress the testpieces using a rotating punch [17], allowing for the deformation mode with pronounced shearing. Although, the theoretical description may be more complicated in this case.

The procedure has been specialized to the yield criterion proposed in [5] using the ring with a hole of an initial radius of 12 mm . Another set of experimental data was obtained using powder compression without a ring. As a result, the functions of the relative density involved in this criterion have been determined. These new functions shown in Eqs. (64) and (65) modify the functions proposed in [5, 16]] to more accurately describe the experimental data. Moreover, the yield stress of the pore-free material has been determined from the same experimental data rather than taken from an independent test on wrought material of the same chemical composition.

The subjects of subsequent investigations will be expanding the experimental program to other materials and ring geometry and identifying other yield criteria.

Author contributions

Conceptualization, S.A. and Y.-M.H.; formal analysis, E.L.; experiment, J.-R.C.; writing—review and editing, S.A. and Y.-M.H. All authors have read and agreed to the published version of the manuscript.

Funding

This research was funded by the Ministry of Science and Technology of the Republic of China (grant number MOST 109-2622-E-110-001–MY3) and the Russian Science Foundation (grant number RSF-23-21-00335).

Acknowledgments

This publication has been supported by the RUDN University Scientific Projects Grant System, project No. 202247-2-000.

Competing interests

The authors declare no financial and non-financial competing interests.

References

[1] B. Druianov, (1993) *"Technological Mechanics of Porous Bodies"*:

[2] S. Alexandrov, (2010) *"Plasticity Theory of Porous and Powder Metals"* **Cellular and Porous Materials in Structures and Processes**: 243–308. DOI: 10.1007/978-3-7091-0297-8_5.

[3] S. Doraivelu, H. Gegel, J. Gunasekera, J. Malas, J. Morgan, and J. Thomas, (1984) *"A new yield function for compressible PM materials"* **International Journal of Mechanical Sciences *26***(9): 527–535. DOI: 10.1016/0020-7403(84)90006-7.

[4] A. A. Benzerga, (2023) *"On the structure of poroplastic constitutive relations"* **Journal of the Mechanics and Physics of Solids *178***: 105344. DOI: 10.1016/j.jmps.2023.105344.

[5] R. Green, (1972) *"A plasticity theory for porous solids"* **International Journal of Mechanical Sciences *14***(4): 215–224. DOI: 10.1016/0020-7403(72)90063-X.

[6] A. L. Gurson, (1977) *"Continuum Theory of Ductile Rupture by Void Nucleation and Growth: Part I—Yield Criteria and Flow Rules for Porous Ductile Media"* **Journal of Engineering Materials and Technology *99***(1): 2–15. DOI: 10.1115/1.3443401.

[7] N. Bilger, F. Auslender, M. Bornert, and R. Masson, (2002) *"New bounds and estimates for porous media with rigid perfectly plastic matrix"* **Comptes Rendus Mécanique *330***(2): 127–132. DOI: 10.1016/S1631-0721(02)01438-9.

[8] A. Maximenko, E. Olevsky, and M. Shtern, (2008) *"Plastic behavior of agglomerated powder"* **Computational Materials Science *43***(4): 704–709. DOI: 10.1016/j.commatsci.2008.01.011.

[9] A. Mbiakop, K. Danas, and A. Constantinescu, (2016) *"A homogenization based yield criterion for a porous Tresca material with ellipsoidal voids"* **International Journal of Fracture *200***(1): 209–225. DOI: 10.1007/s10704-015-0071-9.

[10] T. Dos Santos and G. Vadillo, (2021) *"A closed-form yield criterion for porous materials with Mises–Schleicher–Burzyński matrix containing cylindrical voids"* **Acta Mechanica *232***: 1285–1306. DOI: 10.1007/s00707-020-02925-y.

[11] C. Zheng, H. Wang, Y. Jiang, and G. Li, (2023) *"On the yield criterion of porous materials by the homogenization approach and Steigmann–Ogden surface model"* **Scientific Reports *13***(1): 10951. DOI: 10.1038/s41598-023-38050-8.

[12] P. H. Khavasad and S. M. Keralavarma, (2023) *"Size-dependent yield criterion for single crystals containing spherical voids"* **International Journal of Solids and Structures *283***: 112478. DOI: https://doi.org/10.1016/j.ijsolstr.2023.112478.

[13] A. Cruzado, M. Nelms, and A. Benzerga, (2024) *"Effect of non-uniform void distributions on the yielding of metals"* **Computer Methods in Applied Mechanics and Engineering *421***: 116810. DOI: 10.1016/j.cma.2024.116810.

[14] D. Ichikawa, M. Sawada, and S. Suzuki, (2023) *"The Compression Angle Dependence of the Strength of Porous Metals with Regularly Aligned Directional Pores"* **MATERIALS TRANSACTIONS *64***(10): 2471–2480. DOI: 10.2320/matertrans.MT-M2023055.

[15] L. M. Alves, P. A. Martins, and J. M. Rodrigues, (2006) *"A new yield function for porous materials"* **Journal of Materials Processing Technology *179***(1): 36–43. DOI: 10.1016/j.jmatprotec.2006.03.091.

[16] S. Shima and M. Oyane, (1976) *"Plasticity theory for porous metals"* **International Journal of Mechanical Sciences *18***(6): 285–291. DOI: 10.1016/0020-7403(76)90030-8.

[17] Y.-M. Hwang, S.-K. Yin, H.-C. Yu, and Y.-H. Tsai, (2022) *"Finite element analysis of rotating compression forming of powder materials"* **The International Journal of Advanced Manufacturing Technology *123***(3): 793–807. DOI: 10.1007/s00170-022-10218-y.